PAPER

Check for updates

Green synthesis of PbCrO$_4$ nanostructures using gum of ferula assa-foetida for enhancement of visible-light photocatalytic activity

Rahele Zhiani,[ab] Ali Es-haghi,[c] Seyed Mohsen Sadeghzadeh [ID] *[ab] and Farzaneh Shamsa[ab]

Photocatalytic selective oxidation has attracted considerable attention as an environmentally friendly strategy for organic transformations. Some methods have been reported for the photocatalytic oxidation of sulfides into sulfoxides in recent years. However, the practical application of these processes is undermined by several challenges, such as low selectivity, sluggish reaction rates, requirement of UV-light irradiation, use of additives, and instability of the photocatalyst. Pure monoclinic lead chromate nanoparticles were prepared via a new simple way as Pb and Cr sources. PbCrO$_4$ NPs were synthesized via a green method in the presence of gum of ferula assa-foetida from Pb(NO$_3$)$_2$ and CrCl$_3$ as lead and chromium resources, respectively. The structural analysis of the samples confirmed the formation of PbCrO$_4$ nanostructures in the range of 30 ± 5 nm. The PbCrO$_4$ nanocatalyst was thoroughly characterized by powder X-ray diffraction (XRD), scanning electron microscopy (SEM), transmission electron microscopy (TEM), and energy dispersive X-ray spectroscopy (EDX) study. Considering the large ionic internal character and high mechanical and thermal stability as well as long-term colloidal stability, this system can be considered as a perfect nanocatalyst by using the host–guest approach. A green and ecofriendly method for oxidation of sulfides to sulfones in the presence of O$_2$ as an oxidant was examined for the synthesised PbCrO$_4$ NPs. The easy and applied reusability of the catalyst was observed after the completion of the reaction under visible-light irradiation.

Introduction

The oxidation reaction is one of the most vital protocols for changing raw materials into products.[1–4] Oxidation reactions have some desired features of a 'green' procedure in terms of reduced waste production and play key roles in the industry.[5–9] There are many methods for conventional oxidants for oxidation of sulfide.[10–19] O$_2$ is clean, inexpensive, easily accessible and eco-friendly as its side product is only water. The over-oxidation of sulfides resulting in sulfone formation is a common problem. In this regard, intense efforts have been assigned to the expansion of oxidation reactions using green methods and recyclable catalysts that co-produce safe waste.[20,21] Photocatalytic developments, which use visible light as a great and easily accessible source of energy for catalytic reactions, have been considered to be significant for a sustainable future.[22,23]

There are some reports on the use of molecular oxygen for the photocatalytic oxidation of sulfides into sulfoxides. Chen *et al.* reported photocatalytic systems that exhibited aerobic oxidation of sulfides into sulfoxides by using titanium(IV) oxide as the catalyst.[24–26] These methods used methanol as the solvent, and it was also oxidized to formaldehyde. Also, Li *et al.* conducted photocatalytic oxidation of sulfides on Pt/BiVO$_4$ in water under visible-light illumination.[27]

In the past decades, inorganic nanomaterials have attracted significant interest because of their exclusive properties such as optical, electronic and magnetic properties and potential applications in nanodevices.[28–32] There are four types of reported oxides in Pb–Cr–O ternary system: PbCrO$_4$, Pb$_2$CrO$_5$, Pb$_5$CrO$_8$ and Pb$_{11}$CrO$_{16}$. Three compounds with Pb(PbO)$_n$CrO$_4$ ($n = 0, 1, 4$) composition are known to have optoelectronic properties. PbCrO$_4$ crystallizes in two structures such as stable monoclinic and unstable orthorhombic.[33] PbCrO$_4$ is an important solid material that is applied as a photosensitizer; it has a stable monoclinic structure and is yellow pigment because of its thermal stability and electrical properties.[34] Lead chromate is a significant photocatalyst material. It has been widely applied in decorative and protective systems and mass coloration of fibers, plastics and elastomers.[35,36] Also, lead chromate has been applied as a host material for humidity-sensing resistors, photosensitizers and other devices.[37]

[a]New Materials Technology and Processing Research Center, Department of Chemistry, Neyshabur Branch, Islamic Azad University, Neyshabur, Iran

[b]Young Researchers and Elite Club, Neyshabur Branch, Islamic Azad University, Neyshabur, Iran. E-mail: seyedmohsen_sadeghzadeh@yahoo.com

[c]Department of Biology, Mashhad Branch, Islamic Azad University, Mashhad, Iran

Given our continued interest in nanocatalysis and catalyst development for organic reactions,[38–40] we offer a new, low-temperature and facile route to synthesize nanostructured $PbCrO_4$ utilizing gum of ferula assa-foetida. To the best of our knowledge, it is our first effort to exploit gum of ferula assa-foetida as a novel and renewable catalyst to produce nano-structured $PbCrO_4$. The fuel exploited for the fabrication of the nanostructured $PbCrO_4$ in this research is environmentally friendly and non-toxic. Gum of ferula assa-foetida is rich in ferulic acid as well as disulfite that can play the role of reductant; also, it may be responsible for control over shape and size due to the formation of favorable steric hindrance effect in the synthesis process. The reported method can be easily applied for large-scale production of nanostructured $PbCrO_4$. Therefore, herein, we have used the advantages of the properties of $PbCrO_4$ NPs for the photocatalytic oxidation of sulfide under visible-light irradiation.

Experimental

General procedure for the preparation of $PbCrO_4$ NPs

Here, 0.5 g of lead nitrate and 1.21 g of chromium chloride were dissolved in distilled water. Then, 2 mmol of citric acid was added to the mixed solution and the pH of the above solution was adjusted to 9 by adding tetraethylenepentamine (TEPA) drop-wise; in the next step, 2 mmol of ethylene glycol as the esterification agent was added to the resultant solution. Increasing temperature and evaporation of the gel-like solution led to the preparation of a porous solid mass. One g of gum of ferula assa-foetida was mixed with prepared powders and calcined at 700 °C for 3 h.

General procedure for the oxidation of sulfide

Here, 0.1 mg of $PbCrO_4$ NPs, 3 mmol of thioanisole and 0.1 mmol of triethylamine were added to 5 mL of CH_3OH. After the reaction mixture was stirred for 30 min in dark to reach the adsorption equilibrium, O_2 was purged into the vessel to raise the initial pressure to 0.1 MPa. The reaction mixture was magnetically stirred and illuminated with $\lambda > 400$ nm visible light irradiation at room temperature. At the end of reaction, the $PbCrO_4$ photocatalyst particles were separated from the reaction mixture by filtration and the products were quantitatively analyzed by gas chromatography (GC) equipped with a flame ionization detector (FID) using chlorobenzene as the internal standard.

Compound 2a. Yellow oil, ^{1}H NMR; δ, ppm: 7.68–7.66 (m, 2H), 7.51–7.40 (m, 3H), 2.67 (s, 3H); ^{13}C NMR; δ, ppm: 145.6, 131.0, 129.3, 123.4, 44.1.

Compound 2b. Yellow oil, ^{1}H NMR; δ, ppm: 7.48 (d, $J = 8.2$ Hz, 2H), 7.30 (d, $J = 8.2$ Hz, 2H), 2.67 (s, 3H), 2.38 (s, 3H); ^{13}C NMR; δ, ppm: 142.5, 141.1, 130.0, 123.5, 44.1, 21.4.

Compound 2c. Yellow oil, ^{1}H NMR; δ, ppm: 7.55 (d, $J = 8.7$ Hz, 2H), 7.00 (d, $J = 8.7$ Hz, 2H), 3.76 (s, 3H), 2.65 (s, 3H); ^{13}C NMR; δ, ppm: 161.9, 136.6, 125.2, 114.1, 55.4, 43.8.

Compound 2d. White solid, mp 154–157 °C. ^{1}H NMR; δ, ppm: 8.34 (d, $J = 8.9$ Hz, 2H), 7.88 (d, $J = 8.9$ Hz, 2H), 2.81 (s, 3H); ^{13}C NMR; δ, ppm: 153.1, 149.3, 124.9, 124.3, 44.1.

Compound 2e. Yellow oil, ^{1}H NMR; δ, ppm: 7.61 (d, $J = 8.6$ Hz, 2H), 7.50 (d, $J = 8.6$ Hz, 2H), 2.68 (s, 3H); ^{13}C NMR; δ, ppm: 144.4, 137.3, 129.4, 125.0, 43.9.

Compound 2f. Yellow oil, ^{1}H NMR; δ, ppm: 7.65 (d, $J = 8.4$ Hz, 2H), 7.48 (d, $J = 8.4$ Hz, 2H), 2.70 (s, 3H); ^{13}C NMR; δ, ppm: 145.0, 132.8, 125.3, 124.9, 43.8.

Results and discussion

Crystallite size and respective phase composition of the samples were evaluated by XRD. The crystalline structures of the as-synthesized $PbCrO_4$ NPs were detected by XRD analysis. Fig. 1 shows the XRD pattern of $PbCrO_4$ NPs synthesized with $Pb(NO_3)_2$ and $CrCl_3$. The presence of peaks in the XRD pattern of $PbCrO_4$ is consistent with the monoclinic structure, which is in agreement with JCPDS standard cards no. 08-0210. $PbCrO_4$ belongs to the space group $P2_1/n$ and could be identified in some cases by the (011), (120), and (200) peaks, of which the (011) is most distinct from those of other phases. Also, (120) is the most intense line for $PbCrO_4$. To prove the correct preparation of $PbCrO_4$, EDX pattern was obtained for the sample (Fig. 2). As seen in the spectrum, the sample is composed of Cr, Pb, and O. SEM was used to study the size and morphology of $PbCrO_4$. The SEM image of $PbCrO_4$ showed that the prepared catalyst is nanometer quasi-spherical with an average diameter of 30 ± 5 nm (Fig. 3a). Also, the TEM image of $PbCrO_4$ is presented in Fig. 3b. It clearly shows well dispersion of the prepared catalyst and several larger structures, which can be ascribed to the aggregation/coalescence of each nanoparticle. Table 1 shows the values of BET surface area, pore size, and pore volume for $PbCrO_4$. As for $PbCrO_4$, the BET surface area, total pore volume, and pore diameter (nm) are obtained as 719 m^2 g^{-1}, 2.73 cm^3 g^{-1}, and 24.82 nm, respectively.

Fig. 4 shows the effect of solvent on the catalytic function. The reaction did not proceed in THF or in solvent-free condition and showed low conversion in ethanol and water. Acetonitrile was the best solvent for photocatalytic reactions in certain reports,[41,42] and it also produced a high conversion of 83.9%.
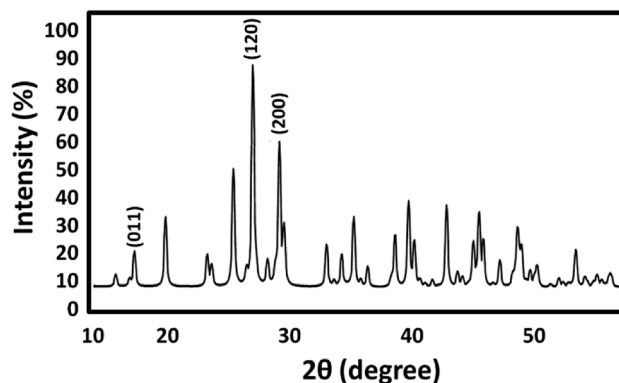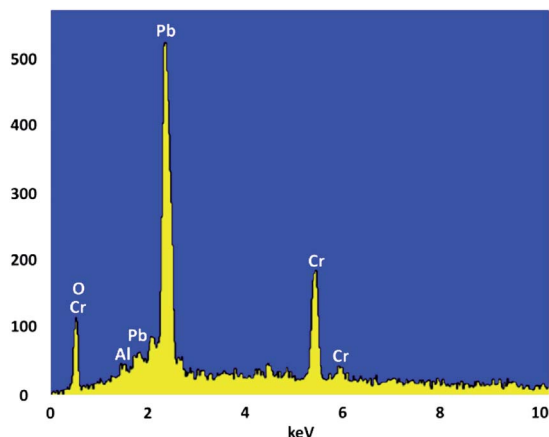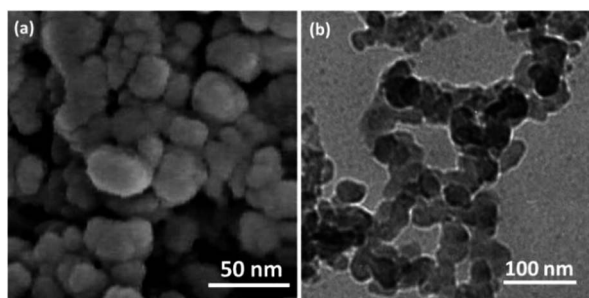

Fig. 1 XRD analysis of $PbCrO_4$ NPs.

Fig. 2 The EDX spectra of PbCrO₄ NPs.

Fig. 3 (a) SEM images of PbCrO₄ NPs; (b) TEM images of PbCrO₄ NPs.

Table 1 Structural parameters of PbCrO₄ NP materials determined from nitrogen sorption experiments

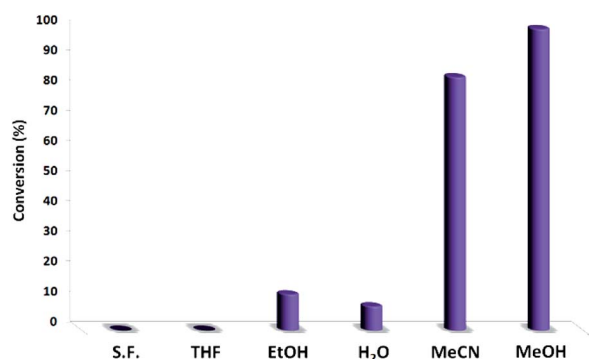| S_{BET} (m^2 g^{-1})	V_a (cm^3 g^{-1})	Pore diameter (nm)
719	2.73	24.82

Fig. 4 Photocatalytic oxidation of sulfides in different solvents.

Methanol resulted in 99.9% conversion. Interestingly, the solvent exhibited a great effect on the photocatalytic activity of PbCrO₄ NPs towards the oxidation of thioanisole. Thus, methanol was selected as a safe solvent.
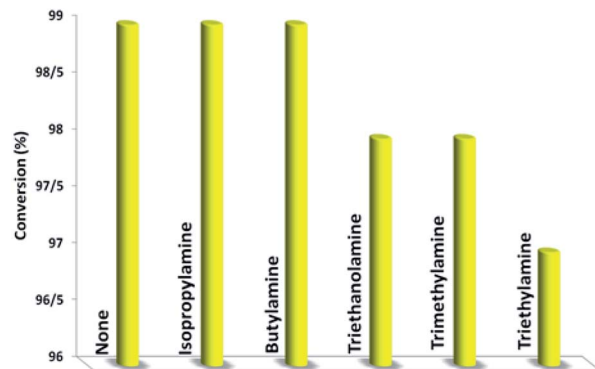

Fig. 5 The influence of amine on the selective aerobic oxidation of thioanisole under visible-light irradiation.
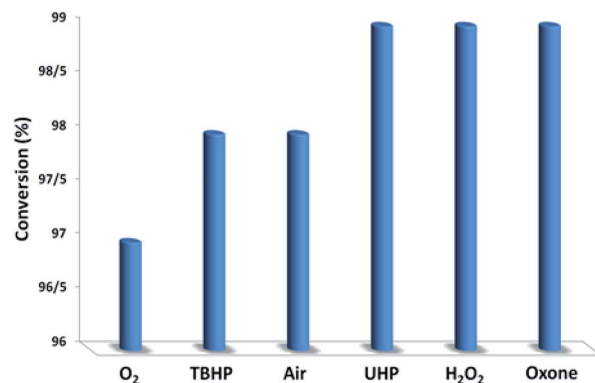

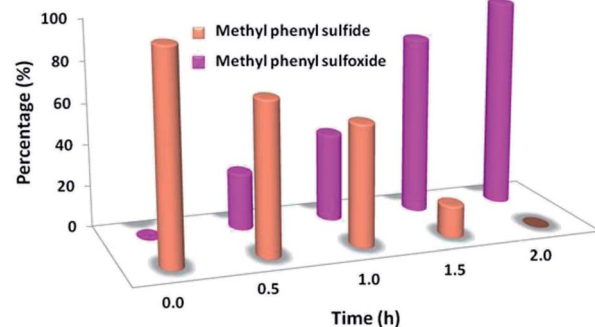**Fig. 6** The screening of the oxidant nature.

Fig. 7 Time course of the product distribution for the photocatalytic oxidation of methyl phenyl sulfide into methyl phenyl sulfoxide.

In the next step, we conducted aerobic sulfide oxidation with a variety of amines, which could be easily separated from the sulfoxide product (Fig. 5). The conversion of thioanisole without amine was very low under visible-light irradiation. Interestingly, with the introduction of amine into the reaction system, the progression of the reaction was significantly boosted. Primary amines can initiate the oxidation, and a decrease in the amount of amine leads to a decrease in the conversion of the product. As expected, the tertiary amines TMA and TEA remained stable
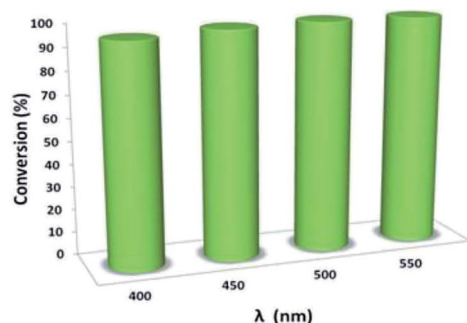
Fig. 8 Control experiment for the synergistic photocatalytic oxidation of thioanisole.
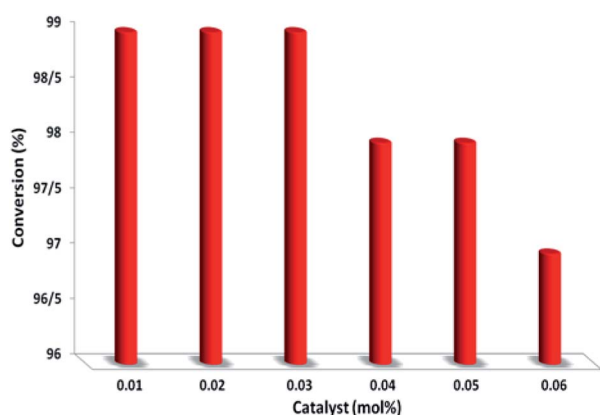

Fig. 9 The effect of catalyst amount.

during the oxidation process, ensuring higher conversions of thioanisole. Based on the data in Fig. 6, common oxidants such as H_2O_2, TBHP, UHP and oxone were weaker oxidants than O_2 for this transformation. During the reaction process, the concentration of methyl phenyl sulfide gradually decreased, whereas the concentration of methyl phenyl sulfoxide gradually increased (Fig. 7). No intermediates or other by-products were observed during the reaction process. After light irradiation for 2 h, methyl phenyl sulfide was quantitatively converted into the target product of methyl phenyl sulfoxide.

Moreover, the reaction shows light-wavelength-dependent behavior. Thus, a wide range of visible-light spectra can be used for this reaction, representing a giant step forward compared to the results obtained in previous reports, where only visible light of approximately 400 nm could be used (Fig. 8).

Table 3 Substrate scope of the oxidation of sulfides into sulfoxides

Entry	Substrate	Product	Conversion [%]
1		(2a)	99.9
2		(2b)	99.9
3		(2c)	99.9
4		(2d)	87.2
5		(2e)	83.9
6		(2f)	86.1

To further prove the catalytic nature of $PbCrO_4$, we varied the amount of $PbCrO_4$ used in the reaction to study its effect on the selective aerobic oxidation of thioanisole under visible-light irradiation; more details and results are summarized in Fig. 9. We discovered that decreasing the amount of $PbCrO_4$ led to a drop in conversion to some extent in comparison with the starting result. Increasing $PbCrO_4$ did not lead to an apparent increase in conversion. These combined results prove that $PbCrO_4$ truly acts as a catalyst for the photoredox process.

In comparison to previously reported methods, our method is milder, greener from viewpoint of oxidant, support, and

Table 2 An overview of some methods for oxidation of thioanisole

Entry	Catalyst	Solvent	Oxidant	T (°C)	t (h)	Yield (%)
1	Na_2WO_4	H_2O	H_2O_2	50	1.0	97 (ref. 43)
2	Ti^{4+}	CCl_4	TBHP	25	9.0	28 (ref. 44)
3	—	MeOH	Oxone	0	0.03	84 (ref. 45)
4	$[WO_4][SiO_2/PrNH_3]_2$	DCM/MeOH	H_2O_2	25	0.5	82 (ref. 46)
5	VO(salen)	DCM	CHP	−20	720.0	79 (ref. 47)
6	$PbCrO_4$	MeOH	O_2	25	2.0	99
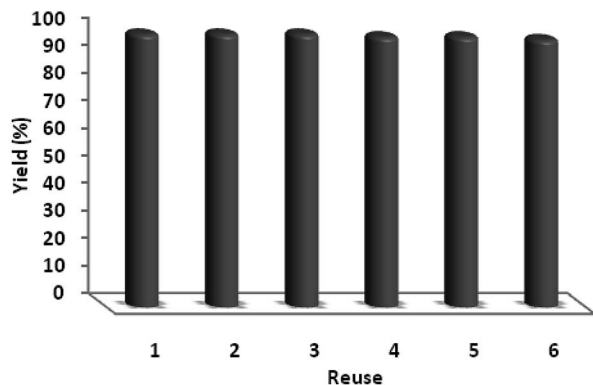
Fig. 10 The reusability of catalysts for the oxidation of thioanisole.

Fig. 11 TEM images of PbCrO$_4$ nano-catalysts after reaction (a). Particle size distribution before reaction (b) and after reaction (c).

metal; it is also cost-effective with higher conversion and selectivity towards production of sulfoxide. This comparison clearly exhibits that our proposed catalyst is excellent (Table 2).

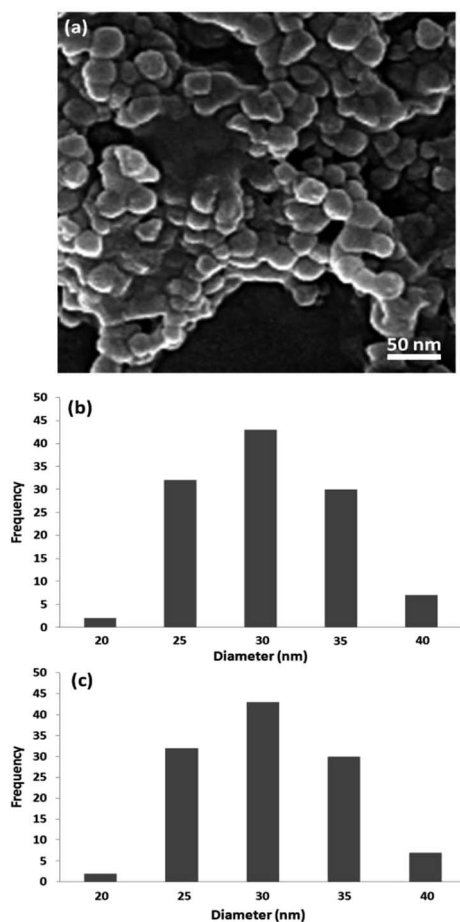After the formulation of tentative reaction mechanism, we finally seek to establish the scope of the substrates for this visible-light photoredox catalysis, which is important for demonstrating the generality of this reaction scheme. The

Scheme 1 Possible mechanism for the visible-light-induced oxidation of sulfides with O$_2$.

reaction results are summarized in Table 3. The sulfides were successfully oxidized into the corresponding sulfoxides with good to excellent yields. The electronic properties of the substituents in the aryl sulfides played an important role in the substrate activity. Generally, the substrates with electron-donating groups demonstrate higher activity than the substrates with electron-withdrawing groups; the latter require longer reaction times to give high yields of the corresponding sulfoxides. The substrates with electron-donating groups more easily donate electrons to sulfur atoms than the substrates with electron-withdrawing groups, which can be beneficial for the oxidation reactions.

One of the most important merits of heterogeneous catalysts is that they can be recycled and reused. Thus, the recyclability of the PbCrO$_4$ catalyst was investigated for the oxidation of thioanisole. After the first catalytic run, the catalyst was separated by centrifugation, leached and washed with water and methanol, and dried at 80 °C under vacuum. The used PbCrO$_4$ catalyst was subjected to a next run under the same conditions. As shown in Fig. 10, the PbCrO$_4$ catalyst demonstrated excellent recyclability. It was recycled six consecutive times with almost unaltered catalytic activity.

The catalytic activity of nano-PbCrO$_4$ depends on the size of the particles, and we observed that PbCrO$_4$ nanoparticles with sizes are effective in catalyzing reactions. However, these nanoparticles generally lose their activity slowly during every reaction cycle. This loss in activity is observed because the nanoparticles grow in size through the Ostwald ripening process, in which small nanoparticles merge together to form large nanoparticles. In the case of the PbCrO$_4$ catalyst system, we observed no appreciable Ostwald ripening, and the particle size and distribution remained the same even after the reaction, which in turn maintained the catalytic activity. Therefore, even after several reaction cycles, the size and distribution of PbCrO$_4$ nanoparticles remain nearly the same (Fig. 11) and thus, the system maintains nearly the same catalytic activity.

The tentative mechanism of visible-light photoredox catalysis by PbCrO$_4$ with triethylamine as a redox mediator is rationalized in Scheme 1. PbCrO$_4$ can absorb a wide range of visible

light. Next, the electron travels through the conduction band of $PbCrO_4$ to react with O_2, thereby forming $O_2^{\cdot-}$. The S-centered free-radical cation prefers to react with $O_2^{\cdot-}$ formed at the conduction band of $PbCrO_4$, allowing the evolution of sulfide peroxide. In the protic solvent CH_3OH, the final methyl phenyl sulfoxide is formed, accompanied by the side products of HCHO and H_2O. At this stage, this proposed mechanism lacks direct evidence (Scheme 1).

Conclusions

In conclusion, $PbCrO_4$ nanoparticles were successfully synthesized via a green method in the presence of gum of ferula assafoetida as a novel nanocatalyst. SEM, TEM, XRD and EDX have been used to characterize the prepared nanocatalyst. Through the photocatalysis of $PbCrO_4$ and TEA, the visible-light-induced selective oxidation of sulfide into sulfoxide with O_2 was successfully conducted in CH_3OH. The interaction between $PbCrO_4$ and TEA gives rise to visible-light activity in the reaction system. This separable solid nanocatalyst can be prepared by a very simple procedure using inexpensive and commercially available precursors, and the catalyst can be reused for six cycles without any loss in its activity as well as composition. Thus, the procedure serves as a valuable alternative in the selective synthesis of sulfoxides.

Conflicts of interest

There are no conflicts to declare.

Notes and references

1 Y. C. Ling, G. M. Wang, J. Reddy, C. C. Wang, J. Z. Zhang and Y. Li, *Angew. Chem., Int. Ed.*, 2012, **51**, 4074–4079.

2 N. Dimitratos, J. A. Lopez-Sanchez and G. J. Hutchings, *Chem. Sci.*, 2012, **3**, 20–44.

3 M. Bordeaux, A. Galarneau and J. Drone, *Angew. Chem.*, 2012, **124**, 10870–10881.

4 S. R. Zhang, L. Nguyen, Y. Zhu, S. H. Zhan, C. K. Tsung and F. Tao, *Acc. Chem. Res.*, 2013, **46**, 1731–1739.

5 R. Blume, M. Hvecker, S. Zafeiratos, D. Techner, A. KnopGericke, R. Schlgl, L. Gregoratti, A. Barinov and M. Kiskinova, *Nanostructured Catalysts: Selective Oxidations*, The Royal Society of Chemistry, 2011, pp. 248–265.

6 J. Piera and J.-E. Bäckvall, *Angew. Chem., Int. Ed.*, 2008, **47**, 3506–3523.

7 F. Geilen, B. Engendahl, A. Harwardt, W. Marquardt, J. Klankermayer and W. Leitner, *Angew. Chem.*, 2010, **122**, 5642–5646.

8 Z. Guo, B. Liu, Q. Zhang, W. Deng, Y. Wang and Y. Yang, *Chem. Soc. Rev.*, 2014, **43**, 3480–3524.

9 T. Matsumoto, M. Ueno, N. Wang and S. Kobayashi, *Chem.–Asian J.*, 2008, **3**, 196–214.

10 P. S. Kulkarni and C. A. M. Afonso, *Green Chem.*, 2010, **12**, 1139–1149.

11 M. V. Gómez, R. Caballero, E. Vázquez, A. Moreno, A. Hoz and Á. Díaz-Ortiz, *Green Chem.*, 2007, **9**, 331–336.

12 B. Karimi, M. Ghoreishi-Nezhad and J. H. Clark, *Org. Lett.*, 2005, **7**, 625–628.

13 R. Noyori, M. Aoki and K. Sato, *Chem. Commun.*, 2003, 1977–1986.

14 K. Sato, M. Aoki and R. Noyori, *Science*, 1998, **281**, 1646–1647.

15 K. Sato, M. Hyodo, M. Aoki, X.-Q. Zheng and R. Noyori, *Tetrahedron*, 2001, **57**, 2469–2476.

16 P. Kowalski, K. Mitka, K. Ossowska and Z. Kolarska, *Tetrahedron*, 2005, **61**, 1933–1953.

17 K. Kaczorowska, Z. Kolarska, K. Mitka and P. Kowalski, *Tetrahedron*, 2005, **61**, 8315–8327.

18 B. M. Choudary, B. Bharathi, C. V. Reddy and M. L. Kantam, *J. Chem. Soc., Perkin Trans. 1*, 2002, 2069–2074.

19 K. Jeyakumar, R. D. Chakravarthy and D. K. Chand, *Catal. Commun.*, 2009, **10**, 1948–1951.

20 C. M. Gordon, *Appl. Catal., A*, 2001, **222**, 101–117.

21 S. Rostamnia, *RSC Adv.*, 2015, **5**, 97044–97065.

22 B. Zhou, J. Song, Z. Zhang, Z. Jiang, P. Zhang and B. Han, *Green Chem.*, 2017, **19**, 1075–1081.

23 W. Huang, B. C. Ma, H. Lu, R. Li, L. Wang, K. Landfester and K. Zhang, *ACS Catal.*, 2017, **7**, 5438–5442.

24 X. Lang, J. Zhao and X. Chen, *Angew. Chem., Int. Ed.*, 2016, **55**, 4697–4700.

25 X. Lang, W. Hao, W. R. Leow, S. Li, J. Zhao and X. Chen, *Chem. Sci.*, 2015, **6**, 5000–5005.

26 X. Lang, W. R. Leow, J. Zhao and X. Chen, *Chem. Sci.*, 2015, **6**, 1075–1082.

27 B. Zhang, J. Li, B. Zhang, R. Chong, R. Li, B. Yuan, S.-M. Lu and C. Li, *J. Catal.*, 2015, **332**, 95–100.

28 S. J. Tans, M. H. Devoret, H. Dai, A. Thess, R. E. Smalley, L. J. Geerligs and C. Dekker, *Nature*, 1997, **386**, 474–476.

29 J. Wang, M. S. Gudiksen, X. Duan, Y. Cui and C. M. Lieber, *Science*, 2001, **293**, 1455–1457.

30 H. Kind, H. Yan, B. Messer, M. Law and P. Yang, *Adv. Mater.*, 2002, **14**, 158–160.

31 J. Hu, T. W. Odom and C. M. Lieber, *Acc. Chem. Res.*, 1999, **32**, 435–445.

32 X. G. Peng, L. Manna, W. D. Yang, J. Wickham, E. Scher, A. Kadavanich and A. P. Alivisators, *Nature*, 2000, **404**, 59–61.

33 K. S. Knight, *Mineral. Mag.*, 2000, **64**, 291–300.

34 S. Vaucher, M. Li and S. Mann, *Angew. Chem., Int. Ed.*, 2000, **39**, 1793–1796.

35 X. L. Hu and Y. J. Zhu, *Chem. Lett.*, 2004, **33**, 880–881.

36 L. J. H. Erkens, H. Hamers, R. J. M. Hermans, E. Claeys and M. Bijnens, *Surf. Coat. Int., Part B*, 2001, **84**, 169–176.

37 K. A. Wishah and M. M. Abdul-Gader, *Appl. Phys. A*, 1998, **66**, 229–234.

38 S. M. Sadeghzadeh, *Appl. Organomet. Chem.*, 2016, **30**, 835–842.

39 M. A. Nasseri and S. M. Sadeghzadeh, *J. Iran. Chem. Soc.*, 2014, **11**, 27–33.

40 S. M. Sadeghzadeh, *Microporous Mesoporous Mater.*, 2016, **234**, 310–316.

41 Z. Chai, T.-T. Zeng, Q. Li, L.-Q. Lu, W.-J. Xiao and D. Xu, *J. Am. Chem. Soc.*, 2016, **138**, 10128–10131.

42 F. Raza, J. H. Park, H.-R. Lee, H.-I. Kim, S.-J. Jeon and J.-H. Kim, *ACS Catal.*, 2016, **6**, 2754–2759.

43 K. Sato, M. Hyodo, M. Aoki, X.-Q. Zheng and R. Noyori, *Tetrahedron*, 2001, **57**, 2469–2476.

44 N. Komatsu, M. Hashizume, T. Sugita and S. Uemura, *J. Org. Chem.*, 1993, **58**, 4529–4533.

45 B. M. Trost and D. P. Curran, *Tetrahedron Lett.*, 1981, **22**, 1287–1290.

46 B. Karimi, M. Ghoreishi-Nezhad and J. H. Clark, *Org. Lett.*, 2005, **7**, 625–628.

47 K. Nakajima, K. Kojima, M. Kojima and J. Fujita, *Bull. Chem. Soc. Jpn.*, 1990, **63**, 2620–2630.